Satellite Color Observations of the Phytoplankton Distribution in the Eastern Equatorial Pacific During the 1982–1983 El Niño

Abstract. *Dramatic changes in the patterns of satellite-derived pigment concentrations around the Galápagos Islands during February and March 1983 are associated with unusual oceanographic conditions observed during the 1982–1983 El Niño. The redistribution of food resources might have contributed to the reproductive failure of seabirds and marine mammals on these islands during this El Niño.*

Nimbus-7 Coastal Zone Color Scanner (CZCS) images (*1*) on 1 and 12 February and 28 March 1983 show the effect of the 1982–1983 El Niño upon the phytoplankton distribution around the Galápagos Islands, located on the equator ~900 km west of South America. Ocean current patterns around islands are complex and in the case of the Galápagos are greatly influenced by the Equatorial Undercurrent (EUC), a subsurface, eastward-flowing current about 200 m thick with its maximum speed normally found at a depth of ~75 m. The circulation is further complicated by the presence at the surface of the shallow (~15 m thick), generally westward-flowing South Equatorial Current (SEC). The CZCS scenes document a major redistribution of phytoplankton around the Galápagos Islands during a period when sea-surface temperatures (SST) were anomalously high (28° to 29°C), the mixed layer was unusually thick (>50 m) for this region, and the winds and both the surface and subsurface flows changed directions.

El Niño is characterized as one of the most spectacular examples of a large-amplitude, interannual response of the ocean to atmospheric forcing. The 1982–1983 El Niño is the best documented event of its kind to date. The pronounced seasonal and year-to-year variability of the near-surface and surface flow and temperature fields are related to changes in the intensity, and sometimes even the direction, of the normally steady southeasterly trade winds. Although variations in the strength of the EUC have been recorded, its presence to the west of the Galápagos Islands was never in doubt until observations (*2*) were made during an El Niño.

Throughout the 1982–1983 El Niño, continuous current measurements (*3*) on the equator were made at only two sites in the Pacific (at 109°30′W and 0°, 95°W). The appearance in August 1982 of anomalous eastward surface flow was one indication that the El Niño had affected the equatorial current system. Normally at this time of year the near-surface flow is westward. This large-scale eastward advection of warm water, combined with a significant reduction of wind-induced upwelling, greatly increased the depth of the mixed layer. By mid-December the top of the thermocline along the equator near the Galápagos Islands was approximately 100 m deep; normally the mixed layer is at a depth of ~15 m (*3*).

Current measurements at 0°, 95°W show (Fig. 1) the changes in the winds and in near-surface and EUC flows during the period covered by the CZCS images. Although the Galápagos Islands lie ~450 km east of the current meter array, these measurements document the dominant oceanic and atmospheric circulation features of the region without the complexity of the islands' interactions. The CZCS patterns observed on any particular day result from a complex set of physical, chemical, and biological processes and responses, which, for the spatial scales and pigment concentrations appropriate to this study, can be expected to have a lag time of between 1 and 2 weeks. For the advective scales the lags could be on the order of 3 to 5 days, and, if there was a biological production rate of one doubling per day, an additional 4 days are probably necessary to support the pigment concentrations observed by the CZCS. From mid-January 1983 on, the core of the EUC disappeared entirely or its strength was about 10 percent of its normal value. Also, the direction of the winds and current flows was generally westward for the period prior to 1 February and eastward before 28 March. The combination of shifting winds and current direction reversals is associated with dramatic changes in the patterns of satellite-derived pigment concentrations.

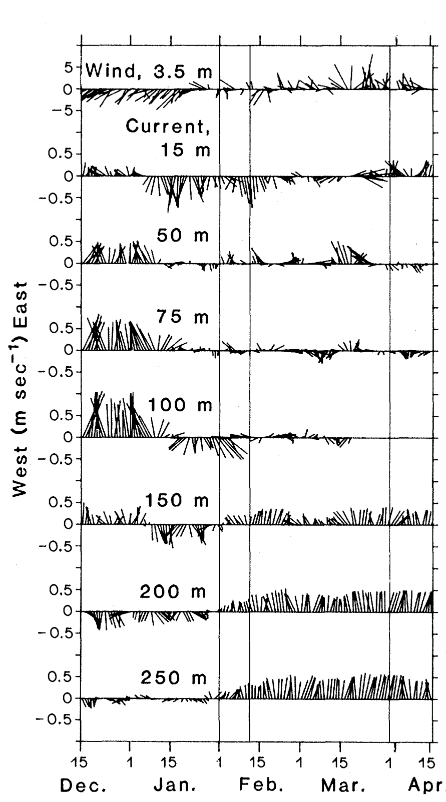

Fig. 1. Daily vector-averaged current vectors (sometimes called "sticks") at 0°, 95°W for depths of 15, 50, 75, 100, 150, 200, and 250 m. The uppermost panel represents wind measurements. The eastward direction is upward.

The CZCS scene on 1 February 1983 (Fig. 2A) (*4*) shows the near-surface pigment distribution after a period of strong westward surface and deeper subsurface (100 to 200 m) flows, when relatively normal southeast trade winds had been observed near the Galápagos and the mixed layer depth was ~60 m. A plume with pigment concentrations greater than 1.5 mg m^{-3} extends ~150 km toward the west from Isabela Island (Fig. 2D). Until about 5 days before the 1 February CZCS observation, the winds were strong and toward the west (Fig. 1), presumably producing vigorous Ekman upwelling. This upward motion and the vertical mixing in the wake of Isabela induced by the westward current flow of the upper ocean probably provide the necessary vertical transport of nutrients into the surface waters to support the observed pigment concentrations. Smaller plumes can also be seen on the western sides of the other islands in the archipelago. The 1 February pigment distributions and concentrations correspond closely with those observed on 24 November 1979 (*5*), when the normal seasonal, non–El Niño environmental characteristics of cool (22°C) surface waters, strong easterly winds, and intense westward SEC flow were observed.

By 12 February 1983, less than 2 weeks later, the CZCS image (Fig. 2B) shows that the pigment distribution around the Galápagos Islands had changed significantly. The winds had been calm and variable in direction and, although westward surface flows continued, periods of weak eastward subsurface flows were recorded (Fig. 1). In general, this had been a quiescent period physically and is reflected in the surface phytoplankton distributions. The plume, with its sharp frontal regions evident on 1 February, has broken down. The geographical area of biological production decreased between 1 and 12 February, and regions of high pigment concentrations are restricted to the northern and southern tips of Isabela Island and to the south of Santa Cruz. The mean pigment concentration for the entire archipelago decreased from 0.30 mg m^{-3} on 1 February to 0.17 mg m^{-3} on 12 February. The ratio of the pigment concentration measured in the western half of the archipelago (*6*) to that observed in the eastern section, however, remained the same (~2.0) on 1 and 12 February.

By the end of March 1983, when the SST was near its maximum for this El Niño (29.5°C), there was a collapse of the trade winds in the eastern Pacific with strong, anomalous westerly winds (Fig. 1). Flow with a dominant easterly component occurred near the surface and was also recorded at 0°, 85°W (*7*). These changing conditions are associated with the drastically altered patterns of pigment distribution around the island archipelago. Streamers of phytoplankton-rich waters extend toward the northeast (Fig. 2C); for example, a large patch, ~60 km in diameter, was observed northeast of Santa Cruz. On the basis of earlier observations of pigment distributions around the Galápagos Islands, the patterns seen in the 28 March 1983 CZCS image are highly unusual. Although the mean pigment concentration (0.28 mg m^{-3}) on 28 March was not significantly different from that on 1 February, there had been a major redistribution between the eastern and western regions; the ratio of the pigment concentration in the western sector to that in the eastern sector was now 0.75. Perhaps as important as the appearance of plumes of phytoplankton-rich water to the east during this phase of the El Niño was the decrease in pigment concentration west of Isabela, normally the most highly productive region in the archipelago. A cross-equatorial transect made along 92°W during March 1983 indicated a 20-fold decrease in absolute primary productivity and a threefold reduction in chlorophyll concentrations compared with normal conditions (*8*).

The dramatic effect of the 1982–1983 El Niño on the phytoplankton distribution ultimately affects the higher trophic levels. Chlorophyll, an indicator of phytoplankton biomass, is not in itself a measure of the abundance of organisms at higher trophic levels. Zooplankton, squid, and fish, however, have been shown to congregate in frontal regions and eddies (*9*). Perhaps it is the persistence of regions of high primary production, rather than the absolute magnitude, that is significant to the higher trophic levels. Fur seals (*Arctocephalus galapagoensis*) on Fernandina Island feed primarily on squid; during this El Niño their foraging time increased from the normal 1 to 2 days to over 5 days, which brought about a deterioration in the physical condition of adults and young (*10*). If the squid were able to maintain themselves within the phytoplankton-rich plumes, then the geographical redistribution seen in Fig. 2 would have made this food resource unavailable to the seals with their geographically restricted foraging range. This redistribution of food resources, combined with a decrease of the primary productivity of the region, might explain the observed reproductive failure of seabirds (*11*) and marine mammals around the Galápagos Islands during the 1982–1983 El Niño (*12*).

GENE FELDMAN
Marine Sciences Research Center, State University of New York, Stony Brook 11794

DENNIS CLARK
National Oceanic and Atmospheric Administration, National Environmental Satellite, Data, and Information Service, Washington, D.C. 20233

DAVID HALPERN
National Oceanic and Atmospheric Administration, Pacific Marine Environmental Laboratory, Seattle, Washington 98115

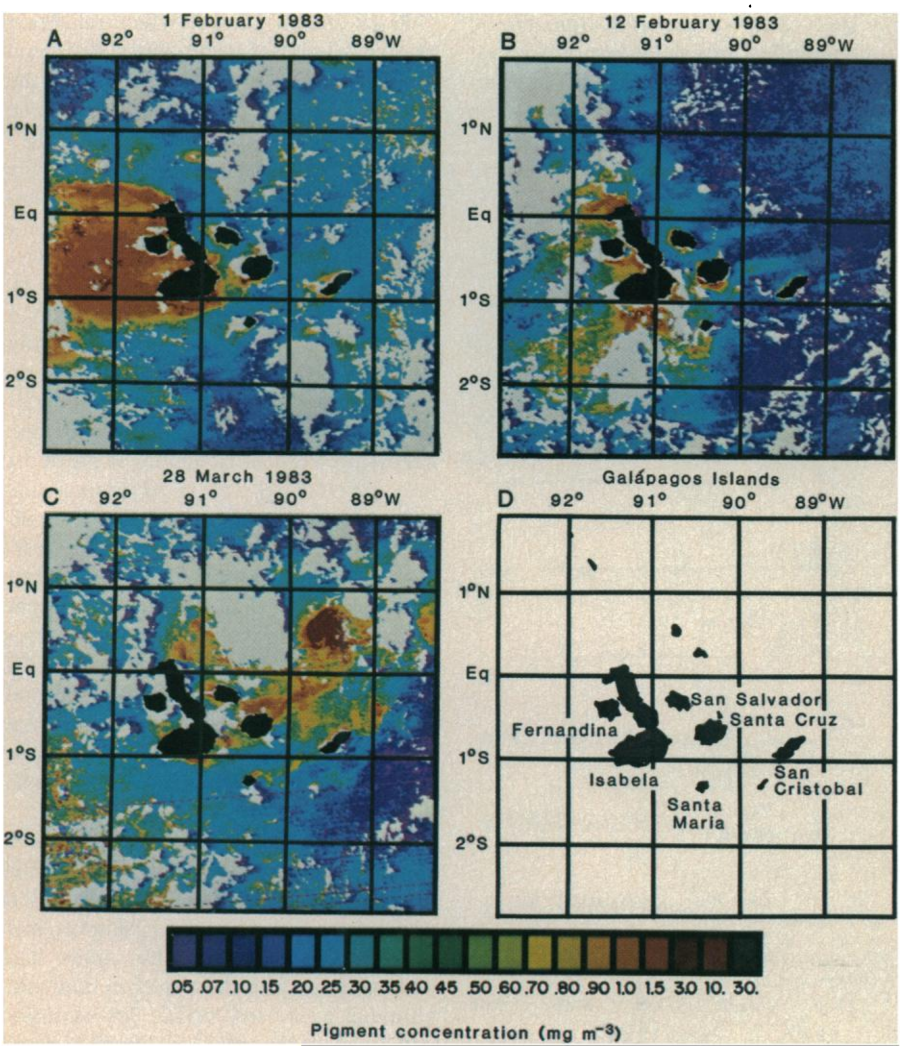

Fig. 2. Color-encoded maps of phytoplankton pigment concentrations acquired on overpasses of the Galápagos Islands (D) derived from Nimbus-7 Coastal Zone Color Scanner imagery on (A) 1 February 1983, orbit 21581; (B) 12 February 1983, orbit 21733; and (C) 28 March 1983, orbit 22341. In this presentation, the major islands are black and the clouds white.

References and Notes

1. The CZCS was designed [W. A. Hovis *et al.*, *Science* **210**, 60 (1980)] to provide quantitative estimates of the near-surface concentrations of phytoplankton pigments based on measurements of the spectral radiance backscattered from the ocean. The subtle variations in water color detected by the CZCS can be directly related to the concentration of phytoplankton pigments (primarily chlorophyll *a* and its associated phaeopigments) over large areas of the ocean (H. R. Gordon, D. K. Clark, J. L. Mueller, W. A. Hovis, *ibid.*, p. 63). Direct comparison between ship-measured and satel-

lite-derived pigment concentrations has demonstrated that the algorithms used to relate the retrieved spectral radiances to phytoplankton pigment concentrations are accurate to within 30 to 40 percent [H. R. Gordon, D. K. Clark, J. W. Brown, O. B. Brown, R. H. Evans, *J. Mar. Res.* **40**, 2 (1982); R. C. Smith and K. S. Baker, *Mar. Biol.* **66**, 269 (1982); C. R. McClain *et al.*, *J. Geophys. Res.* **89**, 3705 (1984).
2. E. Firing, R. Lukas, J. Sadler, K. Wyrtki, *Science* **222**, 1121 (1983).
3. D. Halpern *et al.*, *ibid.* **221**, 1173 (1983).
4. The imagery presented in this report was processed on a satellite data- and image-processing system provided by R. Evans, O. Brown, J. Brown, and A. Lee of the University of Miami, Rosenstiel School of Marine and Atmospheric Sciences.
5. A series of 30 CZCS scenes of the eastern equatorial Pacific beginning in December 1978 and prior to the 1982–1983 El Niño have been examined in an effort to establish the scales of variability observed during normal years.
6. The western region is the area from 91°W to 92°50′W and from 2°S to 1°N; the eastern section is from 89°W to 91°W and from 2°S to 1°N.
7. A. Leetmaa *et al.*, *Trop. Ocean-Atmos. Newsl. No. 21* (1983), p. 11.
8. R. T. Barber and F. P. Chavez, *Science* **222**, 1203 (1983).
9. R. W. Owen, in *Analysis of Marine Ecosystems*, A. R. Longhurst, Ed. (Academic Press, New York, 1981), p. 197.
10. D. Limberger *et al.*, *Trop. Ocean-Atmos. Newsl. No. 21* (1983), p. 16.
11. T. Y. Canby, *Natl. Geogr.* **165**, 144 (1984).
12. A more detailed investigation of the relation between temporal and spatial variability of CZCS-derived phytoplankton distributions and the ecology of the Galápagos Islands is now under way.
13. Research support for G.F. was provided by NASA graduate researchers fellowship grant 33-015-802. We thank W. Hovis and L. Krone for their assistance in the analysis of the historical CZCS data; J. Sissala and P. Anderson for their help in scheduling the CZCS coverage during the 1982–1983 El Niño; R. Barber, J. Kogelschatz, and F. Chavez for their contributions; C. McClain for his support and encouragement; and all our colleagues who provided helpful comments and suggestions on early drafts. The moored measurements were obtained with support from the National Oceanic and Atmospheric Administration's Equatorial Pacific Ocean Climate Study program. Contribution No. 693 from the Pacific Marine Environmental Laboratory, National Oceanic and Atmospheric Administration. Contribution No. 400 from the Marine Sciences Research Center.

6 March 1984; accepted 9 May 1984

Densities of Liquid Silicates at High Pressures

Abstract. *Densities of molten silicates at high pressures (up to ~230 kilobars) have been measured for the first time with shock-wave techniques. For a model basaltic composition (36 mole percent anorthite and 64 mole percent diopside), a bulk modulus* K_s *of ~230 kilobars and a pressure derivative* (dK_s/dP) *of ~4 were derived. Some implications of these results are as follows: (i) basic to ultrabasic melts become denser than olivine- and pyroxene-rich host mantle at pressures of 60 to 100 kilobars; (ii) there is a maximum depth from which basaltic melt can rise within terrestrial planetary interiors; (iii) the slopes of silicate solidi* [(dT_m/dP)*, where* T_m *is the temperature*] *may become less steep at high pressures; and (iv) enriched mantle reservoirs may have developed by downward segregation of melt early in Earth history.*

Knowledge of the properties of silicate liquids at high pressures and temperatures is fundamental to our understanding of the differentiation processes that occur within planetary interiors. Using the falling-sphere technique, Fujii and Kushiro determined the densities of a variety of silicate liquids at up to 20 kbar in a piston cylinder apparatus (*1*). Liquid silicate densities at high pressures have also been calculated by estimation of their elastic properties (*2, 3*). We report here the first shock-wave measurements of the densities of silicate liquids at high temperatures and pressures, extending by more than an order of magnitude (to 235 kbar) the maximum pressure at which the densities have been determined. Our motivations for this work included the following:

1) The rates of melt migration and segregation within partially molten source regions in planetary interiors depend on the difference in density between the melt and the coexisting solids. In addition, the sign of the density contrast between the melt and the coexisting residual crystals determines whether melt will migrate upward or downward (*2*). Magma may move from its source by percolation, in cracks, or as diapirs. In each of these cases, the density contrast between melt and solid enters into the velocity with which the magma moves and thus places important constraints on the thermal and chemical evolution of rising (or sinking) magmas.

2) The slope of the solidus, (dT_m/dP), where T_m is temperature and P is pressure, depends upon ΔV_r (the volume change of the reaction defining the solidus). Thus the pressure dependence of the density contrast between coexisting phases along the solidus is an important factor in the variation of the position of the solidus with pressure and consequently in the melting behavior of planetary mantles.

3) The structures of silicate melts at high pressures and temperatures have been predicted by molecular dynamics simulations. These simulations also model the density and transport properties of silicate melts (*4*). Density measurements at high pressures can be compared with those derived from the simulations to place constraints on the interatomic potentials that are critical to the calculations and hence to refine calculated structural models and transport properties.

The composition that we used for our initial experiments is the 1-atm eutectic composition in the system anorthite-diopside ($An_{0.36}$ $Di_{0.64}$, where the subscripts represent mole fractions). This composition is used as an analog for natural basalt and differs from it mainly in the absence of iron and alkalis. Ultrasonic measurements (*5*) at 1 atm and 1400°C yield a bulk modulus of ~230 kbar for this composition.

The pressure and density (ρ) of a material in shock-wave experiments are determined from the Rankine-Hugoniot equations (*6*). The shock wave is generated in the molten sample encapsulated in molybdenum by impact of a metal flyer plate that has been accelerated to high velocity (1 to 2.5 km/sec) in a 40-mm propellant gun (*7*). A schematic representation of the experimental target, just prior to projectile impact, is shown in Fig. 1 (*8, 9*). During these experiments, the quantities measured are shock velocity (U) and particle velocity (u). One can calculate the 1-atm density (ρ_0) by using partial molar volumes reported by Nelson and Carmichael (*10*). The particle velocity is determined by measurement of projectile velocity and subsequent impedance match with the sample (*9*). One obtains the shock velocity by measuring the time difference between the entrance and exit of the shock front through the sample (*11, 12*).

The results are shown in Table 1 and Fig. 2. The U-u data can be fit by a straight line given by

$$U = (2.94 \pm 0.05 \text{ km/sec}) + (1.29 \pm 0.06)u$$

This experimental fit to the Hugoniot is shown in the inset of Fig. 2. From the analysis developed by Ruoff (*13*), we calculate an isentropic, 1-atm bulk modulus, $K_s^0 = \rho(\partial P/\partial \rho)_s = 226 \pm 8$ kbar, and a pressure derivative, $K_s' = dK_s/dP = 4.15 \pm 0.24$. The value of K_s^0 is in good agreement with the value calculated from the measured ultrasonic velocity (212 to 243 kbar) (*5, 14*). For typical mantle minerals K_s^0 is ~1.2 to 2.1 mbar and K_s' ~4 to 7 (*15*).

With increasing P, crystalline silicates undergo phase changes leading to abrupt increases in ρ as the structure transforms to the closer packing stable at elevated P. Waff (*16*) suggested that similar abrupt increases in ρ would occur in silicate liquids as coordination changes such as ${}^{IV}Al^{3+} \rightarrow {}^{VI}Al^{3+}$ and ${}^{IV}Si^{4+} \rightarrow {}^{VI}Si^{4+}$ occurred. However, silicate liquids could achieve substantial compac-